IEEE Photonics Journal
An IEEE Photonics Society Publication

Open Access

Photonic Integrated Gain Switched Optical Frequency Comb for Spectrally Efficient Optical Transmission Systems

Volume 9, Number 3, June 2017

M. Deseada Gutierrez Pascual, *Student Member, IEEE*
Vidak Vujicic
Jules Braddell
Frank Smyth
Prince Anandarajah, *Senior Member, IEEE*
Liam Barry, *Senior Member, IEEE*

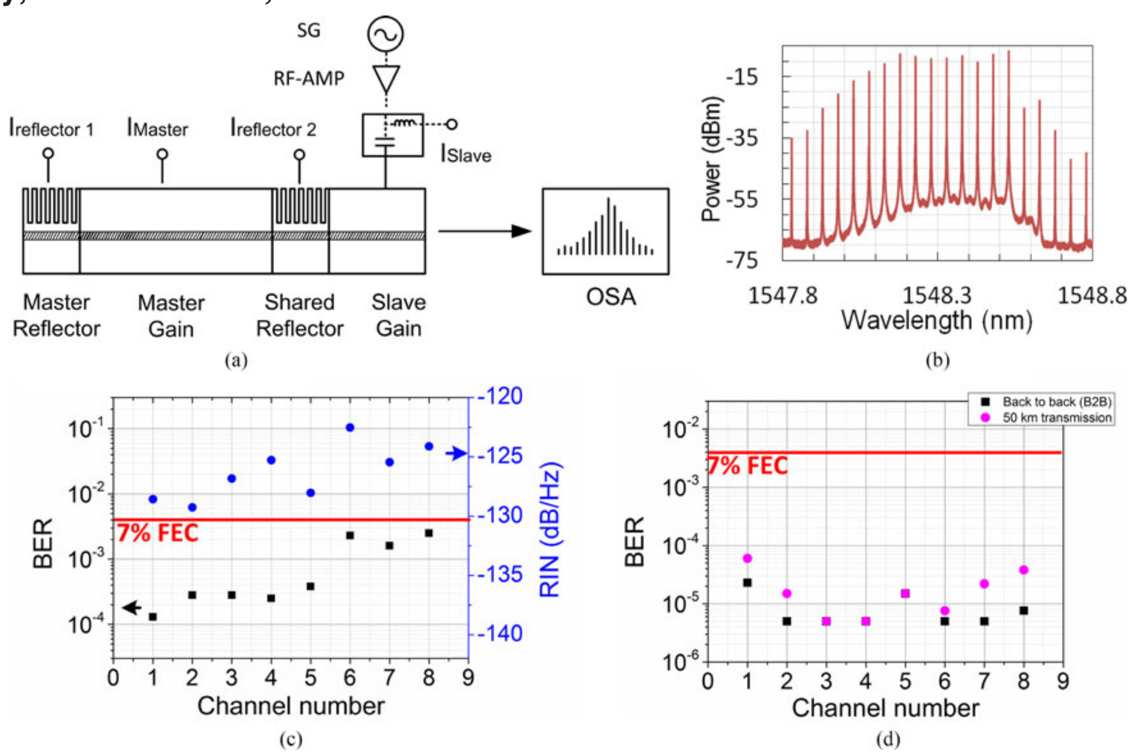

DOI: 10.1109/JPHOT.2017.2678478

Photonic Integrated Gain Switched Optical Frequency Comb for Spectrally Efficient Optical Transmission Systems

M. Deseada Gutierrez Pascual,[1,2] *Student Member, IEEE*, Vidak Vujicic,[1] Jules Braddell,[2] Frank Smyth,[2] Prince Anandarajah,[1] *Senior Member, IEEE*, and Liam Barry,[1] *Senior Member, IEEE*

[1]Department of Electronic Engineering, Dublin City University, Dublin 9, Ireland
[2]Pilot Photonics, Ltd., Invent Centre, Dublin 9, Ireland

DOI:10.1109/JPHOT.2017.2678478

Manuscript received January 18, 2017; revised February 27, 2017; accepted March 2, 2017. Date of current version May 2, 2017. This work was supported in part by the Irish Research Council Employment Based Postgraduate Scheme (EBP-2012), in part by the EU FP7 BIG PIPES (FP7/2007-2013, 619591), in part by the Science Foundation Ireland through the Irish Photonic Integration Centre (12/RC/2276), in part by U.S.-Ireland Programme (15/US-C2C/I3132), and in part by the HEA PRTLI 5 INSPIRE Programs. Corresponding author: M. Deseada Gutierrez Pascual (e-mail: desi@pilotphotonics.com).

Abstract: We demonstrate the performance of a novel integrated gain switched optical frequency comb source (GS-OFCS) in two different optical transmission systems. The device generates a 6.25-GHz frequency spaced comb that comprises eight spectral tones in a 3-dB spectral power ripple. The GS-OFCS presents good noise properties, which include relative intensity noise of ~ -125 dB/Hz and linewidth of 1.5 MHz. We then employ the device in two transmission systems that use advanced modulation formats. First, it is employed in a four-level pulse amplitude modulation format system operating at 3.125-GBaud per channel and over 3 km of standard single mode fiber (SSMF), where all the channels performed below the 7% FEC limit and the receiver sensitivity achieved was -21 dBm. Then, the GS-OFCS is used in a Nyquist quadrature phase-shift keying (QPSK) system at 5-Gbaud per channel and over 50 km of SSMF, where all the channels exhibited a similar performance well below the 7% FEC limit. These results, in conjunction with the compactness and cost efficiency of the integrated device, denote the quality and relevancy of the resultant comb source for future optical transmission systems.

Index Terms: Optical frequency comb, optoelectronic devices, phase shift keying (PSK), photonic integrated circuits, pulse amplitude modulation.

1. Introduction

Data traffic has experienced incessant exponential growth over the last decade due to the appearance of new cloud services and web applications [1], [2]. In order to keep meeting the demand for bandwidth, optical networks must evolve towards higher performance and throughput, spectral efficiency, and reduced power consumption [3], [4]. This significant transformation is required throughout the network, from communications links within datacenters, in metro, and into the backbone [5]–[7].

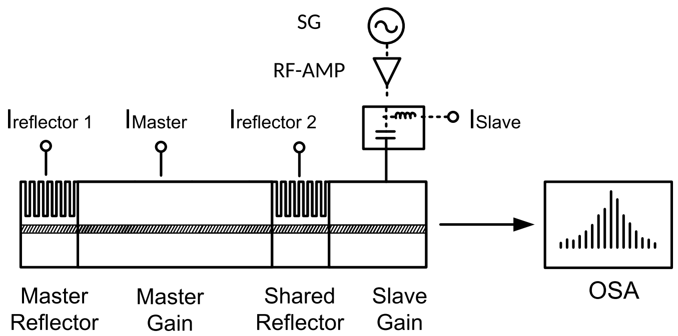

(a)

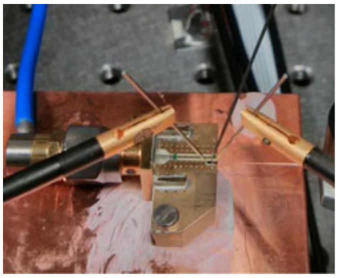

(b)

Fig. 1. (a) Schematic of the photonic integrated device and experimental set up for the gain switched comb generation. (b) PIC under test in a probe station, mounted on a high speed subcarrier that includes an RF connector for gain switching.

Depending on the network topology and application, diverse requirements and specifications (such as transmission lengths, modulation formats and complexity) are stipulated. Transmission links within datacenters are expected to be shorter than 3 km, and while several potential modulation formats have been considered [8]–[10], 4-level pulse amplitude modulation format (PAM-4) has gained remarkable attention [11], [12]. In metro and long-reach links, however, coherent communications are used due to the high receiver sensitivity, frequency selectivity and superiority of digital signal processing (DSP) for compensation of transmission impairments with transmissions lengths over 50 km [13]–[15].

Optical frequency comb sources (OFCS) have proven to be versatile and key components in spectrally-efficient optical transmission systems [14]–[19], thanks to their low complexity, and precise and stable frequency spacing. We focus our work on externally injected gain switched optical frequency comb sources (GS-OFCS) that, as opposed to mode-locked lasers (MLL), offer low relative intensity noise (RIN) unaffected by mode partition noise [17], [19], and low linewidth [20], [21]. Therefore, the GS-OFCS offers itself as a single source with the potential to meet the requirements of various optical networking scenarios from intra-datacenter to long-haul optical transport. Nevertheless, in order to yield further compactness, cost-efficiency and low power consumption, the photonic integration of injected GS-OFCSs is crucial [22].

In this work, we demonstrate the potential of an Indium Phosphide (InP) photonic integrated, externally injected GS-OFCS [23] device for spectrally efficient data transmission systems. The device is composed of two slotted single mode laser diodes with different cavity lengths and integrated in a master-slave configuration. The slave section is optically injected by the master section and simultaneously gain switched. As a result, a 6.25 GHz frequency spaced OFCS consisting of eight comb spectral lines within 3 dB of spectral ripple is obtained. The GS-OFCS is characterized in terms of amplitude and phase noise. The average RIN measured was ~ -125 dB/Hz and the intrinsic optical linewidth corresponded to 1.5 MHz. We then prove the suitability of this GS-OFCS for diverse optical transmission systems that employ multi-level amplitude and phase modulation formats. Hence, the integrated GS-OFCS is used in a PAM-4 and in a Nyquist coherent quadrature phase-shift keying (QPSK) system transmitting over 3 km and 50 km of standard single mode fiber (SSMF), respectively. Both systems performed below 7% FEC limit for all the channels. These experimental results prove that this integrated device is a promising multicarrier source for future communications links that use advanced modulation formats.

2. Photonic Integrated Optical Frequency Comb Source

The fabricated photonic integrated circuit (PIC) for GS-OFCS generation is schematically represented in Fig. 1(a). The overall length of the device is $\sim$1.5 mm, consisting of four electrically

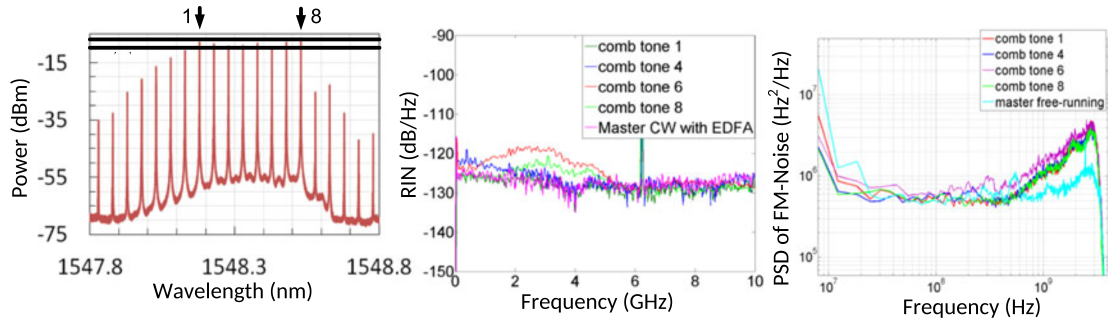

(a) (b) (c)

Fig. 2. (a) Optical spectrum of the photonic integrated gain switched optical frequency comb source (GS-OFCS) with a frequency spacing of 6.25 GHz, presenting eight comb tones in a 3 dB spectral ripple. (b) Relative intensity noise (RIN) for four selected filtered tones over 10 GHz bandwidth. (c) FM-noise spectra for three representative comb tones and free-running master laser.

independent sections. The material structure of the device is a standard 1550 nm laser material with five strained AlGaInAs quantum-wells in the active region, on an n-doped InP substrate.

The comb generator comprises two integrated slotted laser diodes [23] in a master-slave configuration, where the light generated from the master is injected into the slave cavity. These lasers are regrowth free Fabry-Perot lasers that include reflector sections consisting of a number of slots that have been etched close to the active region to provide a regular refractive index perturbation and thus, optical feedback that ensures single mode operation [24]. The reflector on the right end of the master gain section is shared by the slave cavity, effectively reducing the overall length of the PIC. In order to enable gain switching with high speed signals, the PIC was mounted onto a subcarrier that includes an RF connector, a conductor-backed coplanar waveguide (CBCPW) transmission line, and a terminating 47 Ω resistor ball bonded to the slave section for matching impedance. The subcarrier was then placed on a temperature-controlled copper chuck maintained at 20 C for probe testing, as illustrated in Fig. 1(b). The four sections are independently dc biased, with reflector sections biased at 55 mA and the master gain section biased at 80 mA. OFCS generation is achieved by gain switching the slave section with an amplified 6.25 GHz sinusoidal signal (24 dBm) in conjunction with a dc bias of 70 mA applied via a bias tee. The resultant GS-OFCS spectrum can be observed in Fig. 2(a). It exhibits 8 clearly resolved comb lines within 3 dB of spectral ripple, with an optical carrier to noise ratio (OCNR) in excess of 46 dB (RBW = 0.16 pm). The amplitude and phase noise properties of the GS-OFCS are of paramount importance for advanced modulation formats; hence, RIN and phase noise are characterized. The RIN of the master and the selected comb tones used for data transmission has been measured over a 6 GHz bandwidth, although only five measurements are shown in Fig. 2(b) for clarity of presentation. This integrated GS-OFCS presents a relatively uniform RIN over the frequency span, and thereby, it is not affected by mode partition noise unlike some mode-locked lasers comb sources where high RIN is observed at low frequencies which may hinder their use in optical systems [17], [19]. Due to the low power per comb tone after filtering (∼ −24 dBm), an Erbium Doped Fiber Amplifier (EDFA) is required to measure the RIN [22], [25]. Therefore, these measurements are influenced by amplified spontaneous emission (ASE) noise and the actual RIN values for each comb tone are expected to be lower than presented here. The RIN of the master CW (DC to 6 GHz) is −129 dB/Hz. The obtained averaged RIN (DC-6 GHz) of the selected comb tones vary in the range of −122.5 to −129.3 dB/Hz with the highest averaged RIN (−122.5 dB/Hz) corresponding to comb tone 6 that also presents the lowest power and OCNR. This variation in RIN levels can also lead to a degradation of the system performance as it will be presented in the next section. In order to provide a sufficient power per comb line after filtering/demultiplexing for practical systems, an integrated injection locked de-multiplexer [26], [27] can be employed, which provides simultaneous de-multiplexing and amplification of the comb tones while keeping their phase correlation.

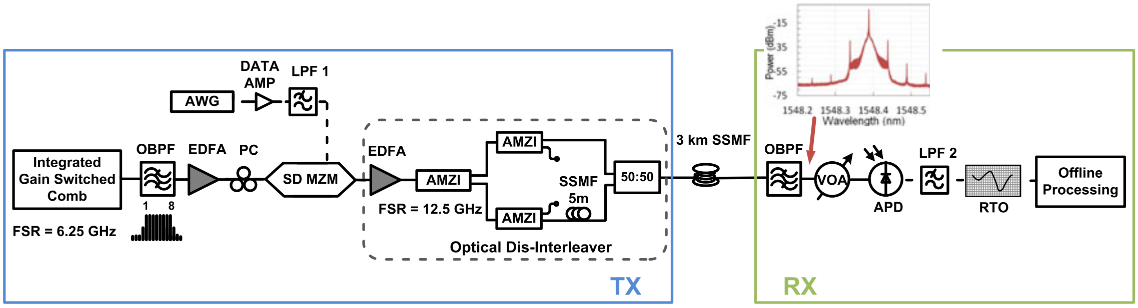

Fig. 3. Schematic of the Nyquist PAM-4 system experimental setup. (Inset) Optical spectrum of a filtered modulated comb tone at the receiver. Free spectral range (FSR); Optical Band-Pass Filter (OBPF); Erbium Doped Fibre Amplifier (EDFA); Polarization Controller (PC); Single-drive Mach Zehnder Modulator (SD-MZM); Arbitrary Waveform Generator (AWG); Data Amplifier (Data Amp); Low Pass Filter (LPF); Asymmetric Mach-Zehnder interferometer (AMZI); Standard Single Mode Fiber (SSMF); Variable Optical Attenuator (VOA); Avalanche Photodetector (APD); Real Time Oscilloscope (RTO).

Finally, we characterize the phase noise properties in detail by measuring the FM-noise spectrum using an optical quadrature front end, as in [28]. The FM-noise spectrum can provide thorough information and understanding of the different noise processes contributing to the overall phase noise, as opposed to the 3 dB optical linewidth which might overestimate the true Lorentzian-shaped linewidth in the presence of abundant low frequency 1/f noise [29].

The FM-noise spectrum was analyzed for the 8 selected comb tones although only four representative measurements are shown in Fig. 2(c). These results are compared to the phase noise of the free-running master laser (when the slave section is biased at transparency current, which allows the master signal to pass through without giving enough gain to the slave laser to emit). As illustrated, the FM-noise spectrum of the master presents a 1/f noise component at low frequencies (below 20 MHz), a clearly dominant white FM noise and a small high-frequency component region above 1 GHz. The intrinsic optical linewidth can be obtained from the white FM-noise component, which corresponds to 1.5 MHz [30]. The FM noise spectra of each comb tone demonstrate similar levels of phase noise, thereby, following the optical linewidth of the master [21], [30]. The excess 1/f noise and relatively high intrinsic optical linewidth will potentially impact the performance in optical coherent systems that will be investigated in Section 4.

3. PAM-4 System Based on the Photonic Integrated GS-OFCS

3.1 Experimental Setup

The experimental setup for the PAM-4 system is illustrated in Fig. 3. The photonic integrated GS-OFCS was used to generate eight optical carriers within 3 dB spectral flatness. As mentioned earlier, all the sections were dc biased accordingly while the slave gain section was also gain switched by employing a high amplitude RF sinewave. The GS-OFCS was filtered to select the central eight optical carriers and suppress the outer side comb tones. All the filtered comb tones were subsequently amplified with an EDFA and sent to a single-drive Mach-Zehnder modulator (SD-MZM) via a polarization controller (PC). The SD-MZM was biased at the quadrature point and then used to modulate the filtered comb with an amplified 3.125 GBaud PAM-4 signal waveform. An arbitrary waveform generator (AWG, Tektronix AWG70002A) operating at 6.25 GSa/s was employed to generate the PAM-4 signal which was then amplified and sent through a low-pass filter (LPF 1) with a passband of 2.5 GHz. The PAM-4 signal waveform was 2^{16} bits long and pre-distorted to compensate for nonlinearities of the data driver and the SD-MZM. Therefore, the bandwidth of the optical 3.125 GBaud PAM-4 signal was 5 GHz, and there is a 1.25 GHz guard band between adjacent optical channels. The modulated eight-channel PAM-4 signal was de-correlated by passing through a two-stage dis-interleaver based on asymmetric Mach-Zehnder interferometers (AMZI), with an FSR of 12.5 GHz to separate the comb into odd and even channels with an extinction ratio

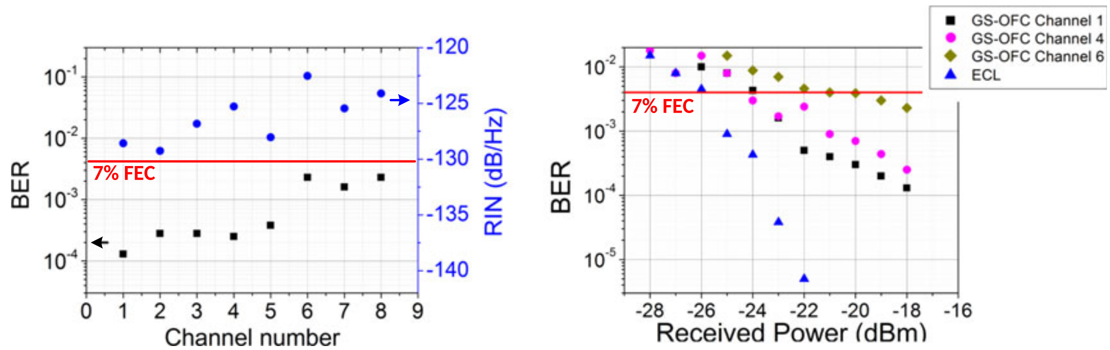

(a) (b)

Fig. 4. (a) Measured BER for selected channels after transmission over 3 km. (b) BER as a function of received power after 3 km transmission.

of 30 dB. The even channels were passed through a 5 m fiber patch cord for de-correlation and then, passively combined with the odd channels for transmission over 3 km of SSMF.

At the receiver side, the desired channel was selected with a narrowband tunable optical band-pass filter (OBPF) Yenista STM-50 with an approximate 3 dB bandwidth of 6 GHz. The optical spectrum of a filtered modulated comb tone is shown in inset in Fig. 3. The filtered channel was detected using a 10 GHz receiver that consists of an avalanche photodetector (APD) and an integrated trans-impedance amplifier. A variable optical attenuator (VOA) was used to vary the input power falling on the APD to measure bit error rate (BER) as a function of the received optical power. The detected signal was filtered using a 5 GHz LPF (LPF 2) and captured with a real time oscilloscope (RTO) operating at 25 GSa/s. Digital processing of the received signal (resampling, normalization, adaptive equalization, symbol synchronization, decoding), and BER calculations were performed offline using Matlab. The adaptive equalizer was a 13 tap finite impulse response (FIR) filter, and the tap weights were updated using decision-directed least-mean square (DD-LMS) algorithm [31]. The symbol synchronization was performed with the aid of a 2^5 symbols long training sequence.

3.2 Results and Discussion

The performance of the 50 Gbit/s PAM-4 system after 3 km SSMF transmission was verified by carrying out BER measurements. Fig. 4(a) illustrates the BER achieved (black squares) for a received optical power of ~ -18 dBm, and the corresponding RIN for each channel (blue circles). The performance for all the received filtered channels are below the 7% FEC (BER $= 3.8 \times 10^{-3}$ [32]) limit. It can be observed that the performance tends to degrade for higher channel number due to the reduction of OCNR and increase of the RIN, which are key performance limiting factors of multi-level amplitude modulation formats [17], [19] such as PAM-4. Hence, the best performance with a BER of 1.3×10^{-4} corresponds to Channel 1 that exhibits a low RIN of -128.6 dB/Hz. On the contrary, the worst BER of 2.3×10^{-3} is incurred by Channel 6 that presents the lowest OCNR and highest RIN of -122.5 dB/Hz. We then analyze the BER as a function of received power for three representative channels. An ECL was used to set a benchmark performance of the system, as shown in Fig. 4(b) with blue triangles. The ECL has an average RIN (DC-6 GHz) of ~ -145 dB/Hz, and OCNR in excess of 65 dB (RBW $= 0.16$ pm). Consequently, the penalty in performance for the GS-OFCS channels is caused by elevated RIN (ranging -122.5 to -129.3 dB/Hz) and inferior OCNR compared to the ECL. Channel 1 to 5 exhibit a similar level of performance yielding a receiver sensitivity of -23 dBm, corresponding to 2 dB power penalty at 7% FEC limit compared to the ECL. Channel 6 to 8 present a receiver sensitivity of -21 dBm at the 7% FEC limit. The additional 2 dB penalty incurred by these channels are mainly attributed to the degradation in RIN values and

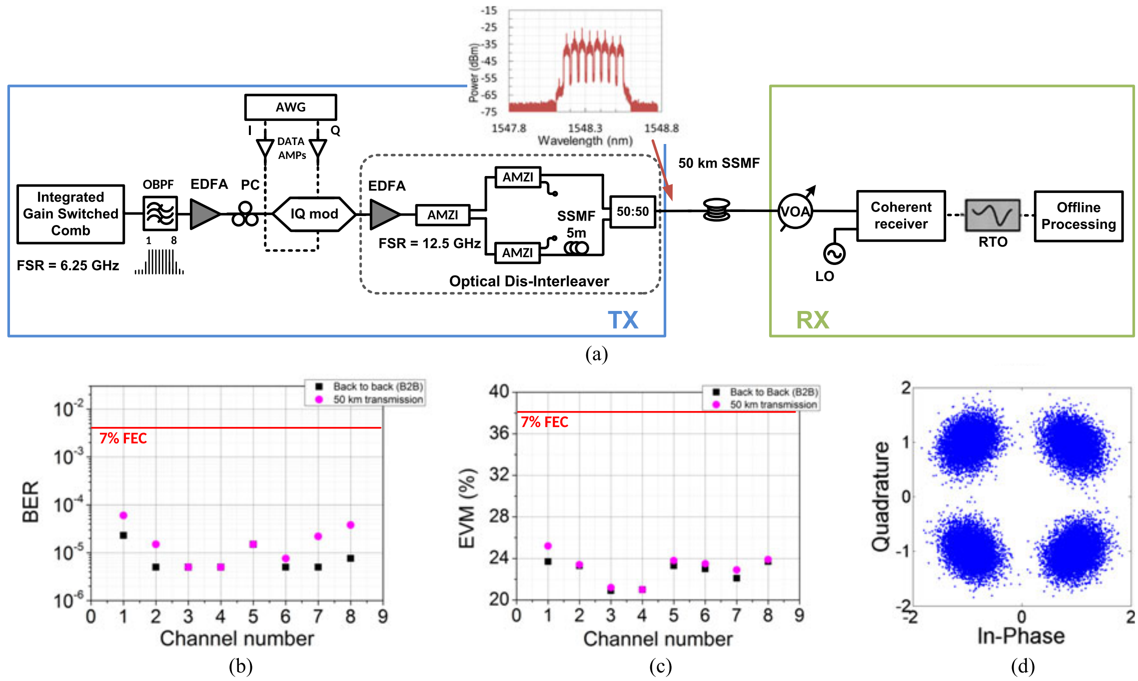

Fig. 5. (a) Schematic of the Nyquist-QPSK system experimental setup. (Inset) Optical spectrum of the modulated superchannel prior transmission; IQ Mach-Zehnder modulator (IQ mod); Local Oscillator (LO). (b) Measured BER for selected channels back-to-back (black squares) and after transmission over 3 km of SSMF (magenta circles). (c) Measured EVM for selected channels back-to-back (black squares) and after transmission over 3km of SSMF (magenta circles). (d) QPSK constellation diagram for Channel 7.

OCNR of these channels. Nevertheless, these results have clearly illustrated the feasibility of a PAM-4 system utilizing the proposed photonic integrated GS-OFCS device.

4. Coherent Nyquist-QPSK System Based on the Photonic Integrated GS-OFCS

4.1 Experimental Setup

Fig. 5 illustrates the experimental setup for the Nyquist-QPSK system. The photonic integrated GS-OFCS was used as the multicarrier source. An OBPF and an EDFA were employed to select and amplify the central 8 optical carriers with a 3 dB spectral flatness. All the filtered comb tones were sent to a single IQ Mach-Zehnder modulator (IQ-mod) via a polarization controller (PC). The IQ-mod was biased at null and driven by a 5 GBaud Nyquist-QPSK signal waveform. The waveform was 2^{16} bits long and derived from the same AWG used previously, operating at 25 GSa/s. A digital root raised cosine filter with a roll-off factor of 0.1% was applied to the QPSK signal. The bandwidth of the resulting Nyquist-QPSK signal was 5 GHz with a 1.25 GHz guard band between adjacent optical channels. The signal was then passed through the de-correlation stage, as explained in detail in Section 3.1 of this article, and transmitted back-to-back (B2B) and over 50 km of SSMF. At the receiver side, a phase diversity coherent receiver was used to perform coherent detection. The optical local oscillator (LO) was provided by an ECL that had 13 dBm output power and 25 kHz optical linewidth. The LO was tuned to each of the 8 channels for detection. The received signal was captured with a RTO operating at 25 GSa/s. Digital processing of the received signal (timing deskew, resampling, adaptive equalization, matched filtering, frequency offset compensation, carrier phase recovery and phase tracking), was performed offline using Matlab. A second-order PLL [33], [34] was used for phase recovery and phase tracking. Channel performance was determined using error-vector magnitude (EVM) calculation of the measured constellation diagrams, as well as error counting to establish a bit error rate.

4.2 Results and Discussion

The experimental results obtained are shown in Fig. 5(b) and (c), for the total received optical power (received power of the entire eight-channel Nyquist-QPSK signal) of ~ -25 dBm. Fig. 5(b) shows the BER measurements for each channel and for back-to-back case (black squares) and for transmission over 50 km of SSMF (magenta circles). We evaluate 2 million samples for each channel to accurately estimate the BER. Channel performance was also analyzed through EVM measurements for each channel for back-to-back case and for transmission over 50 km of SSMF, as illustrated in Fig. 5(c). In both cases, all eight channels exhibit a similar performance far below the 7% FEC limit (BER $= 4 \times 10^{-3}$ and EVM $=$ 38% [35]). Channels 3 and 4 had the best performance in B2B and 50 km transmission. An indicative measured constellation diagram for Ch. 7 is shown in Fig. 5(d). The constellation diagrams of all channels present a slightly angular spread of the constellation points which is a distinct signature of phase noise. Despite the relatively large linewidth (relative to the employed baud rate), these experimental results demonstrate that this integrated comb source can be used in coherent systems, even at low baud rates where the linewidth requirement is more stringent.

5. Conclusion

We report on the implementation of a photonic integrated gain switched comb source in two different spectrally efficient optical transmission systems. The device comprises two lasers with different cavity lengths integrated in a master-slave configuration. The generated comb presents eight clearly resolved and highly coherent optical tones spaced by 6.25 GHz within a 3 dB spectral window and an OCNR of at least 45 dB. The comb noise properties of the individual comb tones are analyzed by characterizing the RIN and phase noise which are key parameters for advanced modulation formats. Average RIN is found to be ~ -125 dB/Hz and an intrinsic optical linewidth of 1.5 MHz is characterized. We investigate the performance of the integrated comb source in a PAM-4 and in a Nyquist QPSK transmission system. In the PAM-4 system, we investigate the performance of the device by modulating eight comb tones with a 3.125 Gbaud signal that is subsequently transmitted over 3 km of SSMF. We show that the performance for all the received channels is below the 7% FEC limit but it tends to degrade for high channel number due to inferior OCNR and RIN characteristics, with a 2 dB receiver sensitivity penalty between channels. In the Nyquist-QPSK system we also study the device phase noise influence. We modulate eight comb tones with a 5 GBaud Nyquist-QPSK signal and transmit it over 50 km of SSMF. Successful transmission is achieved with all eight channels exhibiting a similar performance far below the 7% FEC limit (BER $= 4 \times 10^{-3}$ and EVM $=$ 38%). These results highlight the suitability of this integrated GS-OFCS for future spectrally efficient transmission systems that rely on advanced modulation formats. Furthermore, this compact InP monolithically integrated device provides further simplicity, ease of manufacture, and reduced footprint of future transmitters. Future work will strive for higher frequency spacing for these integrated devices, as achieved using discrete components [36], to allow higher data throughput and transmission. Finally, by optimizing the device design, we expect to achieve increased output power and to reduce the RIN and phase noise.

References

[1] Cisco V. N. I. Forecast, “Cisco visual networking index: forecast and methodology 2013-2018,” 2016. [Online]. Available: http://www.cisco.com/c/en/us/solutions/collateral/service-provider/ip-ngn-ip-next-generationnetwork/white_paper_c11-481360.html

[2] R. J. Essiambre and R. W. Tkack, “Capacity trends and limits of optical communication networks,” *Proc. IEEE*, vol. 100, no. 5, pp. 1035–1055, May 2012.

[3] S. Gringeri, E. B. Basch, and T. J. Xia, "Technical considerations for supporting data rates beyond 100 Gb/s," *IEEE Commun. Mag.*, vol. 50, no. 2, pp. 21–30, Feb. 2012.
[4] A. A. M. Saleh and J. M. Simmons, "Technology an architecture to enable the explosive growth of the Internet," *IEEE Commun. Mag.*, vol. 49, no. 1, pp. 126–132, Jan. 2011.
[5] C. Kachris and I. Tomkos, "A survey on optical interconnects for data centers," *IEEE Commun. Surveys Tut.*, vol. 14, no. 4, pp. 1021–1036, Oct. 2012.
[6] R. P. Davey and D. B. Payne, "The future of optical transmission in access and metro networks an operator's view," in *Proc. 31st Eur. Conf. Opt. Commun.*, 2005, Glasgow, U.K., 2005, vol. 5, pp. 53–56.
[7] P. Winzer, "Beyond 100G ethernet," *IEEE Commun. Mag.*, vol. 48, no. 7, pp. 26–30, Jul. 2010.
[8] Q. Hu, D. Che, Y. Wang, and W. Shieh, "Advanced modulation formats for high-performance short-reach optical interconnects," *Opt. Exp.*, vol. 23, no. 3, pp. 3245–3259, Feb. 2015.
[9] L. Tao, Y. Ji, J. Liu, A. P. T. Lau, N. Chi, and C. Lu, "Advanced modulation formats for short reach optical communication systems," *IEEE Netw.*, vol. 27, no. 6, pp. 6–13, Nov./Dec. 2103.
[10] M. J. Wale, "Advanced modulation formats in data centre communications," in *Proc. 2nd Symp. Opt. Interconnects Data Centres*, Cannes, France, Sep. 2014, pp. 1–13.
[11] F. Karinou *et al.*, "Directly PAM-4 modulated 1530-nm VCSEL enabling 56 Gb/s/λ data-center interconnects," *IEEE Photon. Technol. Lett.*, vol. 27, no. 17, pp. 1872–1875, Sep. 2015.
[12] D. Sadot, G. Dorman, A. Gorshtein, E. Sonkin, and O. Vidal, "Single channel 112 Gbit/sec PAM4 at 56 Gbaud with digital signal processing for data centers applications," *Opt. Exp.*, vol. 23, pp. 991–997, Jan. 2015.
[13] D. Lavery, E. Torrengo, and S. Savory, "Bidirectional 10 Gbit/s long-reach WDM-PON using digital coherent receivers," in *Proc. Opt. Fiber Commun. Conf./Nat. Fiber Opt. Eng. Conf.*, 2011, Paper OTuB4.
[14] J. Pfeifle *et al.*, "Flexible terabit/s Nyquist-WDM super-channels using a gain-switched comb source," *Opt. Exp.*, vol. 23, pp. 724–738, Jan. 2015.
[15] V. Ataie *et al.*, "Ultrahigh count coherent WDM channels transmission using optical parametric comb-based frequency synthesizer," *IEEE J. Lightw. Technol.*, vol. 33, no. 3, pp. 694–699, Feb. 2015.
[16] C. Weimann *et al.*, "Silicon-organic hybrid (SOH) frequency comb sources for terabit/s data transmission," *Opt. Exp.*, vol. 22, no. 3, pp. 3629–3637, 2014.
[17] V. Vujicic *et al.*, "Quantum dash mode-locked lasers for data centre applications," *IEEE J. Sel. Topics Quantum Electron.*, vol. 21, no. 6, pp. 53–60, Dec. 2015.
[18] J. Pfeifle *et al.*, "Coherent terabit communications with microresonator Kerr frequency combs," *Nature Photon.*, vol. 8, no. 5, pp. 375–380, 2014.
[19] V. Vujicic *et al.*, "Mitigation of relative intensity noise of quantum dash mode-locked lasers for PAM4 based optical interconnects using encoding techniques," *Opt. Exp.*, vol. 25, pp. 20–29, 2017.
[20] P. M. Anandarajah *et al.*, "Generation of coherent multicarrier signals by gain switching of discrete mode lasers," *IEEE Photon. J.*, vol. 3, no. 1, pp. 112–122, Feb. 2011.
[21] M. D. Gutierrez Pascual, R. Zhou, F. Smyth, P. M. Anandarajah, and L. P. Barry, "Software reconfigurable highly flexible gain switched optical frequency comb source," *Opt. Exp.*, vol. 23, no. 18, pp. 225–235, Aug. 2015.
[22] M. D. Gutierrez, J. Braddell, F. Smyth, and L. P. Barry, "Monolithically integrated lasers for comb generation in bandwidth variable transponders," in *Proc. 18th Eur. Conf. Integr. Opt.*, Warsaw, Poland, 2016, Paper o01.
[23] M. D. Gutierrez, V. Vujicic, J. Braddell, F. Smyth, P. Anandarajah, and L. P. Barry, "InP photonic integrated externally injected gain switched optical frequency comb," *Opt. Lett.*, vol. 42, no. 3, pp. 555–558, 201.
[24] C. Herbert *et al.*, "Discrete mode lasers for communication applications," *IET Optoelectron.*, vol. 3, no. 1, pp. 1–17, Feb. 2009.
[25] Eagleyard-Photonics, "Relative intensity noise of distributed feedback lasers," 2016. [Online]. Available: http://www.eagleyard.com/fileadmin/downloads/documents/eyP_App_Note_RIN__1-6.pdf
[26] A. Albores-Mejia, T. Kaneko, E. Banno, K. Uesaka, H. Shoji, and H. Kuwatsuka, "Optical-comb-line selection from a low-power/low-OSNR comb using a low-coherence semiconductor laser for flexible ultra-dense short range transceivers," in *Proc. Opt. Fiber Commun. Conf.*, 2015, Paper W2A.23.
[27] M. D. Gutierrez, J. Braddell, F. Smyth, and L. P. Barry, "Monolithically integrated 1x4 comb de-multiplexer based on injection locking," presented at the European Conf. Integrated Optics, Warsaw, Poland, pp. 1–2, 2016.
[28] K. Shi *et al.*, "Dynamic linewidth measurement method via an optical quadrature front end," *IEEE Photon. Technol. Lett.*, vol. 23, no. 21, pp. 1591–1593, Nov. 2011.
[29] T. N. Huynh *et al.*, "200-Gb/s baudrate-pilot-aided QPSK/Direct detection with single-section quantum-well mode-locked laser," *IEEE Photon. J.*, vol. 8, no. 2, Apr. 2016, Art. no. 7903107.
[30] R. Zhou, T. N. Huynh, V. Vujicic, P. M. Anandarajah, and L. P. Barry, "Phase noise analysis of injected gain switched comb source for coherent communications," *Opt. Exp.*, vol. 22, pp. 8120–8125, Mar. 2014.
[31] D. Smalley, "Equalization concepts: A tutorial," Texas Instruments, DAllas, TX, USA, Appl. Rep. SPRA140, Oct. 1994.
[32] N. Eiselt *et al.*, "Evaluation of real-time 8x56.25 Gb/s (400G) PAM-4 for inter-data center application over 80 km of SSMF at 1550 nm," *IEEE J. Lightw. Technol.*, vol. 35, no. 4, pp. 955–962, Oct. 2016.
[33] T. N. Huynh, A. T. Nguyen, W. C. Ng, L. Nguyen, L. A. Rusch, and L. P. Barry, "BER performance of coherent optical communications systems employing monolithic tunable lasers with excess phase noise," *IEEE J. Lightw. Technol.*, vol. 32, no. 10, pp. 1973–1980, May 2014.
[34] V. Vujicic *et al.*, "Tbit/s optical interconnects based on low linewidth quantum-dash lasers and coherent detection," in *Proc. Conf. Lasers Electro-Opt.*, San Jose, CA, USA, 2016, Paper SF2F.4.
[35] R. Schmogrow *et al.*, "Error vector magnitude as a performance measure for advanced modulation formats," *IEEE Photon. Technol. Lett.*, vol. 24, no. 1, pp. 61–63, Jan. 2012.
[36] P. Anandarajah *et al.*, "Flexible optical comb source for super channel systems," in *Proc. Opt. Fiber Commun. Conf./Nat. Fiber Opt. Eng. Conf.*, 2013, Paper OTh31.8.